Global biodiversity patterns of marine forests of brown macroalgae

Fragkopoulou, E., Serrão E. A., De Clerck O., Costello M. J., Araújo M. B., Duarte C. M., Krause‐Jensen D., & Assis J.

Published in: Global Ecology and Biogeography
DOI: 10.1111/geb.13450

Available online: 17 Jan 2022

Citation:
Fragkopoulou, E., Serrão E. A., De Clerck O., Costello M. J., Araújo M. B., Duarte C. M., Krause‐Jensen D., & Assis J. (2022). Global biodiversity patterns of marine forests of brown macroalgae. Global Ecology and Biogeography, 31, 636–648. doi: 10.1111/geb.13450

Global biodiversity patterns of marine forests of brown macroalgae

Eliza Fragkopoulou[1*], Ester A. Serrão[1], Olivier De Clerck[2], Mark John Costello[3], Miguel B. Araújo[4,5], Carlos M. Duarte[6,7], Dorte Krause-Jensen[6,8], Jorge Assis[1]

[1]CCMAR- Center of Marine Sciences, University of the Algarve, 8005-139 Faro, Portugal

[2]Phycology Research Group, Biology Department, Ghent University, Krijgslaan 281 (S8), 9000 Ghent, Belgium

[3]Faculty of Bioscience and Aquaculture, Nord Universitet, Postboks 1490, Bodø 8049, Norway.

[4]Department of Biogeography and Global Change, National Museum of Natural Sciences, CSIC, Calle José Gutiérrez Abascal, 2,28806 Madrid, Spain

[5] Rui Nabeiro Biodiversity Chair, MED - Mediterranean Institute for Agriculture, Environment and Development, University of Évora, Largo dos Colegiais, 7000 Évora, Portugal

[6]Arctic Research Centre (ARC), Aarhus University, Ole Worms Allé 1, 8000 Århus C, Denmark

[7]Red Sea Research Center (RSRC) and Computational Bioscience Research Center (CBRC), King Abdullah University of Science and Technology (KAUST), Thuwal, Saudi Arabia

[8]Department of Bioscience, Aarhus University, Vejlsøvej 25, 8600 Silkeborg, Denmark

*Corresponding author

Short running title: Biodiversity patterns of brown macroalgae

Abstract

Aim Marine forests of brown macroalgae create essential habitats for coastal species and support invaluable ecological services. However, their global biodiversity patterns are insufficiently

understood to provide an overall perspective on their biogeography and conservation priorities. This study maps species richness and endemicity patterns of brown macroalgae at global scales.

Location Global

Time period Contemporary

Major taxa studied Marine forests of brown macroalgae, here defined as kelp (orders Laminariales, Tilopteridales, Desmarestiales) and fucoid (order Fucales) inhabiting subtidal and intertidal environments

Methods We coupled a large dataset of macroalgal observations (420 species) with a high-resolution dataset of relevant environmental predictors (i.e., light, temperature, salinity, nitrate, wave energy, ice coverage) to develop species distribution models (SDMs). We stacked models across species (stacked-SDMs) to develop global species richness and endemicity estimates.

Results Temperature and light were the main predictors shaping the distribution of subtidal species, while wave energy, temperature and salinity were the main predictors of intertidal species. Highest regional species richness for kelp was found in the North East Pacific (maximum 32 species) and for fucoids in South East Australia (maximum 53 species), supporting the hypothesis that these regions were the evolutionary sources for colonization of the world by brown macroalgae. Locations with low species richness coincided between kelp and fucoid, occurring mainly at higher latitudes (e.g., Siberia) and the Baltic Sea, where extensive ice-coverage and low-salinity regimes prevail. Regions of high endemism for both groups were identified in the Galapagos Islands, Antarctica, South Africa and East Russia.

Main conclusions Geographical patterns and environmental predictors of species richness differ between kelp and fucoids, suggesting that their distinct ecological niches were shaped by past environmental conditions at their source regions of lineage evolution. Our extensive mapping of

47 species richness and endemism provides a global perspective of priority regions for conservation of
48 brown macroalgae forest diversity.
49
50 **Keywords:** biodiversity patterns, brown macroalgae, endemism, fucoid, kelp, macroecology, marine
51 forests, species richness, stacked-species distribution models
52

53 Introduction

54 Global species richness and endemicity patterns are the outcome of evolutionary and ecological
55 processes driven by large-scale geological events and long-term climate characteristics and
56 fluctuations (Wiens & Donoghue, 2004). Understanding and estimating these patterns has been a
57 longstanding challenge, yet it remains a fundamental step in ecological, evolutionary and
58 conservation studies (Costello et al., 2017; Tittensor et al., 2010). Contemporary changes in species
59 richness driven by human-induced pressures can however rapidly alter patterns that would
60 otherwise have been shaped across evolutionary time (Pecl et al., 2017). In the marine environment,
61 such recent changes in the distributions of species and calls for protecting 30% of the oceans raised
62 the need to assess global biodiversity patterns, namely the location of rich-spots of species richness
63 and centres of endemicity.
64
65 Species richness and endemism are fundamental metrics of biodiversity and indicators of high
66 conservation value; however, their regional patterns do not necessarily overlap (Costelo et al., 2017;
67 Kerswell, 2006; Selig et al., 2014). Our current knowledge of marine species richness gradients and
68 endemicity centres remains heavily biased towards specific taxa and regions (e.g., Selig et al., 2014;
69 Taheri et al., 2021; Tittensor et al., 2010). For the majority of the studied marine taxa (mostly fish,
70 mammals, corals and bivalves) species richness follows a latitudinal bimodal distribution, with

peaks varying geographically between clades (Chaudhary et al., 2016; Kusumoto et al., 2020; Lin et al., 2020). Although centres of high marine endemicity, mostly islands including Japan and the Galapagos, or climate-locked continental regions such as South Africa and South Australia, have been identified and are common across clades, they can still differ between taxa (Costello et al., 2017; Harrison & Noss, 2017; Kier et al., 2009; Selig et al., 2014). Geographic biases in data have impaired proper estimates of biodiversity baselines for more taxonomic groups and regions. While recent online repositories containing large amounts of data (e.g., OBIS – Ocean Biogeographic Information System, GBIF – Global Biodiversity Information Facility) have opened new opportunities to broaden our knowledge of distributional patterns for a wider spectrum of marine species (e.g., Chaudhary et al., 2016; Costello et al., 2017; Kusumoto et al., 2020; Selig et al., 2014), they are still incomplete and may contain spatial and taxonomic errors (e.g., Assis et al., 2020). Global diversity patterns for brown macroalgae are one such geographically biased example, with many studies concentrated in a few geographical regions, despite their key importance in providing ecosystem services. For such marine macroalgal forests, the distribution of global species richness and endemicity centres have to date been poorly understood due to insufficient and / or unreliable data at global scales (Costello et al., 2017).

Macroalgae can form dense and complex marine forest habitats that provide habitat to numerous associated species, increase local biodiversity, and support ecosystem services including food provision and security, shoreline protection from wave energy, nutrient cycling and carbon fixation (e.g., Arafeh-Dalmau et al., 2020; Coleman & Wernberg, 2017; Krause-Jensen et al., 2018; Wernberg et al., 2019). Despite their importance, there are only a handful of studies addressing global patterns at the species level, restricted to limited taxa of the orders *Bryopsidales* (green algae) and *Dictyotales* (brown algae), mainly due to the lack of reliable data and poor taxonomic resolution (Kerswell,

2006; Verbruggen et al., 2009; Vieira et al., 2021). Additional studies on global macroalgal richness and endemicity patterns were conducted, but only at the genus level, which is not necessarily representative of the species patterns (Keith et al., 2014; Kerswell, 2006). Besides, distinct lineages of macroalgae are expected to have distinct richness and endemicity patterns, reflecting their evolutionary histories, as is the case of fucoid versus kelp brown algae (e.g., Bringloe et al., 2020).

This study aims to estimate global patterns of species richness of brown macroalgae, identify endemicity centres and explore the underlying environmental drivers shaping distributions. To address and overcome the information challenges and gaps highlighted above, we fitted species distribution models (SDMs; Anderson et al., 2011) and stacked them (Guisan & Rahbek, 2011). The models used a machine learning algorithm to examine the relationship between biologically relevant predictors (Assis et al., 2017a; Fragkopoulou et al., 2021) and occurrence records derived from a recently published large dataset of marine forests of kelp (a common name that here designates Laminariales, Tilopteridales, Desmarestiales) and fucoid (Fucales) macroalgae. The dataset provides information from multiple sources (online repositories, literature and herbaria), and was quality-controlled for spatial and taxonomical errors (Assis et al., 2020). This approach allowed us to produce biodiversity estimates per taxonomic group, accounting for dispersal and ecological constraints (Mendes et al., 2020). Our results provide global maps and environmental limits of regions with distinct levels of species diversity and endemicity for kelp and fucoid. This novel global and digital information is the baseline for planning and prioritising locations for biodiversity conservation and management (e.g., Zhao et al., 2020).

Methods

Occurrence records and environmental data

Occurrence records of kelp (Orders Laminariales, Tilopteridales and Desmarestiales) and fucoid (order Fucales) were gathered from the curated dataset of marine forests (Assis et al., 2020). The dataset contains observations largely matching the time window of the environmental predictors (~80% records after 2000; see next paragraph; Assis et al., 2020). After removing species with less than 5 occurrence records (van Proosdij et al., 2016), the initial 531 species of interest were pruned to a final dataset of 420 species (113 species of kelp and 307 fucoid).

A set of biologically relevant environmental predictors for near present-day conditions was extracted from Bio-ORACLE (long-term average climatologies between 2000 and 2017) for the benthic (i.e., along the seafloor) and intertidal realms (surface layers), depending on whether species have subtidal or intertidal distributions (Assis et al., 2017b; Tyberghein et al., 2012). Light availability, temperature (minimum and maximum), nitrate, salinity and sea ice coverage were selected as potential predictors for both subtidal (i.e., benthic data) and intertidal (i.e., surface data) macroalgae, and the additional low altitude cloud fraction and maximum air temperature were added to intertidal fucoids (i.e., surface data). Moreover, maximum wave energy was included as a potential predictor for both intertidal and subtidal macroalgae, to account for high-energy environments. This layer was produced to match the Bio-ORACLE 5 arcmin resolution with the nearest neighbour algorithm based on the classification developed by Fairley et al., (2020). Wave energy is provided in 6 classes, with 1 representing enclosed seas with calm conditions and 6 the highest-energy oceanic coasts, influenced by large, long period swells and storm conditions (Fairley et al., 2020). Prior to modelling, collinearity between predictors was assessed with Pearson's correlation coefficient as well as the Variance Inflation Factor (VIF; Araújo et al., 2019; Harisena et al., 2021). If high correlation was found between predictor pairs, only one would be included in the models.

Stacked-Species Distribution Models (stacked-SDMs)

Individual distribution models at the species level (SDMs) were produced with Boosted Regression Trees (BRT, De'ath, 2007), a machine learning algorithm that combines the advantages of regression trees and boosting, fits complex non-linear relationships between response (occurrence data) and predictor variables (environmental data), and provides high predictive performance (Assis et al., 2017a; Elith et al., 2006; Fragkopoulou et al., 2021). Moreover, proper hyper-parametrization (e.g., number of trees, learning rate, etc.) and the ability to force monotonicity responses strongly reduced overfitting of BRT and therefore increased the potential for transferability (Elith et al., 2008; Hofner et al., 2011). A minimum number of 1000 pseudo-absences or the same number as presences (if more than 1000) were randomly generated in sites where no presences of the species were recorded (Barbet-Massin et al., 2012), and were geographically limited to the provinces (Spalding et al., 2007) where the species occurs as well as their neighbouring provinces (Araújo et al., 2019). This limited pseudo-absences to regions where no records of the species were found, but where dispersal could occur, which is a crucial step in SDM development (Assis et al., 2017a; Barve et al., 2011).

To reduce surplus information as well as the negative effect of autocorrelation in the models (Dormann et al., 2007), the correlation of predictors within the range of occurrence records (presence and pseudo-absences) was tested as a function of geographic distance. For this purpose, correlograms were built to pinpoint the minimum distance at which predictors were significantly correlated. Records per species were pruned by randomly selecting one record from the pool found within such distances (e.g., Assis et al., 2017a; Fragkopoulou et al., 2021).

Models fitted records per species (presences and pseudo-absences) against predictor variables, and hyper-parametrization was optimized through cross-validation by partitioning data into 6 independent latitudinal bands. In this process, models were interactively trained with all hyperparameter combinations (i.e., the "grid search" method) of number of trees (50 to 1000, at steps of 50), learning rate (0.01 and 0.001) and tree complexity (1 to 6, at steps of 1). Predictive performance of the models was evaluated in one latitudinal band withheld at a time with the area under the curve (AUC) of the receiver operating characteristic curve (Fielding & Bell, 1997). The optimal hyperparameter combination that reduced overfitting and increased transferability, was found as the one that produced models with higher AUC in cross-validation (Assis et al., 2017a; Vignali et al., 2020). The cross-validation framework also allowed inferring the final performance of the models tuned with the optimal hyperparameters in independent data (Assis et al., 2017a; Fragkopoulou et al., 2021; Vignali et al., 2020). Overfitting was further controlled through the forcing of specific monotonic responses to the predictors (i.e., negative or positive influence; Hofner et al., 2011). Negative monotonic responses were set for maximum temperature, ice coverage and maximum wave energy, and positive for the remaining environmental predictors.

The relative contribution of predictors to the models was determined by computing the increase in AUC when each predictor was added to its alternative model (i.e., the one including all predictors except that being tested). Apparent physiological tolerance limits (maximum and minimum, depending on the predictor) were estimated from individual response functions produced for each predictor, while fixing all alternative predictors to their averages (Assis et al., 2017a; Elith et al., 2008). Final models for prediction were built by discarding predictors with residual or negative

contributions through a stepwise approach based on AUC. To this end, a full model was fitted (i.e., with all predictors) and predictors were interactively removed one at the time, from the least to the higher contributive, until the difference of AUC between the full model and the reduced model was higher than zero (Elith et al., 2008; Fragkopoulou et al., 2021). This resulted in parsimonious models (i.e., with fewer predictors), which tend to be more robust to the effects of multicollinearity in the data (Dormann et al. 2013) and have occasionally been shown to have higher spatial and temporal transferability (Randin et al., 2006; Sequeira et al., 2018; but see for a more thorough evaluation of the trade-offs between model complexity and predictive power, García-Callejas & Araújo, 2016).

Maps reflecting the potential distribution and environmental suitability for each species were developed for global shorelines with the selected parsimonious models. These maps were reclassified into binomial surfaces reflecting the presence and absence of suitable habitats for the species, by applying a threshold maximizing both specificity (true negative rate) and sensitivity (Fielding & Bell, 1997).

To account for dispersal constraints, maps were clipped to suitable reachable area, an approach that reduces potential overprediction, with no increase in underprediction (Thuiller et al., 2004; Mendes et al., 2020). This assumes that a species might not cross potential barriers with unsuitable conditions, such as land and ocean basins, unless demonstrated by occurrence records (Ballesteros-Mejia *et al.*, 2017). Final predictive performance was assessed with AUC and True Skill Statistic (TSS; Allouche et al., 2006) for both maps clipped and unclipped to reachable areas.

Potential species richness was inferred for kelp and fucoid forests by stacking predictions from individual distribution models with a sum function (i.e., binary stacked species distribution models; Guisan & Rahbek, 2011). Because species richness estimates are scale dependent (Kusumoto et al., 2020), we inferred the optimal resolution of the standardized Uber's hexagonal hierarchical spatial data (Bondaruk et al., 2019) by computing the average difference between observed and predicted species richness at each resolution of hexagon shapes. The Uber's hexagonal framework was chosen due to its equal-area projection and optimal indexing algorithm, which allows fast data aggregation over its hierarchical resolutions (Bondaruk et al., 2019). Further, the local (i.e., per hexagon) species range-rarity was quantified as a measure of endemism by the corrected endemism index (CWEI; Crisp et al., 2001; Schmitt et al., 2017). The weighted endemism index (WEI; 1) for the hexagon c was calculated by summing the inverse of the geographical range size $r_{i,c}$ for each of the n_c species. In this way, species with a smaller geographical range were assigned a larger weight. To reduce correlation between species richness and endemism, the corrected endemism index $CWEI_c$ (2) was calculated as the weighted endemism index WEI_c divided by the total number of species RS_c found within each hexagon c (Crisp et al., 2001; Schmitt et al., 2017).

$$\mathrm{WEI}_c = \sum_{i=1}^{n_c} \frac{1}{r_{i,c}} \quad (1) \qquad\qquad \mathrm{CWEI}_c = \frac{\mathrm{WEI}_c}{\mathrm{RS}_c} \quad (2)$$

Results

The final dataset for which individual species distribution models were produced, comprised 113 kelp (628,425 occurrence records) and 307 fucoid species (383,958 records). Of these, 36 were

intertidal (Table S1). Models achieved high performance in predicting species occurrence for both kelp (cross-validation AUC: 0.87 ± 0.07; AUC: 0.98 ± 0.02; TSS: 0.92 ± 0.07) and fucoids (cross-validation AUC: 0.95 ± 0.08; AUC: 0.98 ± 0.01, TSS: 0.93 ± 0.07; Table S2).

The performance of the models significantly improved for kelp and fucoids after accounting for dispersal constraints across unsuitable habitats, i.e., clipping to suitable reachable areas (Significant increase for kelp: ΔAUC: 0.02 ± 0.01, ΔTSS: 0.06 ± 0.02; Significant increase for fucoid: ΔAUC: 0.02 ± 0.01, ΔTSS: 0.06 ± 0.03; Wilcoxon signed-rank test).

The distribution of the subtidal kelp and fucoid species was best explained by light and extreme temperature (minimum and maximum) at the seafloor (relative average contributions >10%; Figure 1). Intertidal distributions were best explained by wave energy, temperature (minimum and maximum) and salinity (relative average contributions >10%; Figure 1). Nitrate concentration and sea ice coverage had a lower (~5-10%; Figure 1) contribution to the models, yet the distribution limits of some species were strongly shaped by thresholds defined by these predictors (95th percentile of contributions 19% - 38% for both subtidal and intertidal species; Figure 1). Cloud fraction and maximum air temperature showed a low contribution to the models for intertidal species (contributions ~5%; Figure 1; Table S3). These findings are reinforced by the overall low collinearity between predictors (Table S4); as only minimum and maximum ocean temperatures showed stronger collinearity for subtidal species, while collinearity was also found between maximum air and sea temperatures for intertidal species (Pearson's Correlation > 0.85; VIF > 5; S4). However, their opposite monotonic fit in BRT (negative for maximum temperatures and positive for minimum temperatures) allowed removing confounding inferences about the contribution of predictors.

Physiological thresholds, inferred from partial dependency plots for each environmental predictor (Figure 2), were, for kelp biome, 2.7ºC and 23.7ºC (95th percentile -1.8ºC and 32.5ºC) for thermal tolerance (long-term average of minimum and maximum temperatures across species) and 0.24 E m^{-2} y^{-1} minimum light. Subtidal fucoids showed higher estimated thermal tolerance thresholds, 9.4ºC and 28.7ºC (95th percentile -1.8ºC and 34.9ºC), and higher minimum light, above 1.11 E m^{-2} y^{-1}. In contrast, intertidal fucoids, showed lower thermal tolerances, 2.5ºC and 22.8ºC (95th percentile between -1.8ºC and 28.6ºC), maximum wave energy of class 5 (95th percentile between 1 and 6) and minimum salinity above 16 (95th percentile between 3.3 and 34.6; Table S3).

Stacking individual SDMs to unique layers allowed the estimation of potential species richness distribution patterns. The optimal resolution of the global grid system based on Uber hexagon shapes was 60 km edge length (Figure 3). At this resolution, the average difference between observed and predicted species richness was 0.96 (i.e., we predicted 0.96 species more than observed), with a Pearson correlation of 0.85 (Figure 3). This 60 km optimal resolution scale was then used to aggregate regional species richness and endemicity estimations for kelp (Figure 4) and fucoid forests (Figure 5) from the model predictions.

Overall, suitable habitat area estimated for kelp (1,705,227 km^2) was smaller than for fucoids (2,574,986 km^2), but the two groups had some overlap in suitable regions (Table S5). Species richness patterns differed latitudinally, with peaks of diversity in distinct regions for kelp and fucoids and overall endemicity regions coinciding, although with some differences between the two groups (Figure 4; Figure 5).

Kelp exhibited a latitudinal bimodal species richness distribution, with a minimum near the equator and peaks between 13-77º in the northern and 5-64º in the southern hemisphere (Figure 4a). The highest regional species richness (32 species) was found in the North East Pacific, with numerous regional rich-spots from Alaska to Baja California. In the northern hemisphere, additional rich-spots occurred in the Atlantic regions of Greenland to Newfoundland and from Norway to Portugal; followed by fewer rich-spots in the West Pacific, from the Okhotsk Sea to South Korea. In the southern hemisphere, species richness was lower (maximum 10 species) and the richest regions were South-East Australia and around New Zealand. Regions of low kelp species richness (i.e., poor-spots) were predicted at higher latitudes (1-2 species), but extended along large areas, such as in North and South America and North Russia, associated with ice-driven or river-discharges salinity minima. Smaller-sized poor-spots were predicted in the warm regions of the Mediterranean, the Red Sea and South China (Figure 4a). Highest kelp endemicity was predicted in the Galapagos Islands, Peru, Chile, Brazil, Falkland Islands, Antarctica, South Africa, Heard Island and McDonald Islands and East Russia (Sakhalin and Kuril Islands; Figure 4b; Table S6).

Fucoid species diversity was distributed from 171º North to 64º South (Figure 5a). The highest regional richness (53 species) was predicted in South Australia with numerous rich-spots from Brisbane to Kalbarri. Additional rich-spots were predicted in New Zealand, in the Indo-Pacific (Indonesia), North-West Pacific along the coasts of Japan and Guangdong China, North Atlantic from Norway to Morocco, around Iceland and along the Newfoundland coast (Figure 5a). Poor-spots were mostly predicted in the South-East Pacific (Chile), the South-East Mediterranean and the Black Sea. Fucoid endemicity was predicted in Hawaii, Baja California, the Galapagos Islands and continental Ecuador, Antarctica, South Africa, Red Sea and Arabian Peninsula, South China,

Japan, East Russia (Sakhalin and Kuril Islands), South East Australia and New Zealand (Figure 5b; Table S7).

Discussion

We estimated the global distribution of species richness and endemicity for marine forests of kelp and fucoids; a goal previously hindered by insufficient or unreliable data. The geographic centres of species richness here identified differed between groups and were strongly driven by thermal affinities. For kelp, highest species richness was found in the North East Pacific (up to 32 species) and for fucoids in South East Australia (up to 53 species). These rich-spots differ from those previously identified for the predominantly tropical macroalgae orders Bryopsidales (Indo-Australian Archipelago; Kerswell, 2006) and Dictyotales (Central Indo-Pacific; Vieira et al., 2021), and even differed within each order between intertidal and subtidal species, consistent with the geography of their evolutionary origin. In contrast, poor-spots of species richness coincided between kelp and fucoids (e.g., higher latitudes; Figure 4a; Figure 5a), in line with previous studies (Kerswell, 2006; Vieira et al., 2021). Coinciding regions of species endemicity for kelp and fucoids were identified in the Galapagos Islands, Antarctica, South Africa, Japan and East Russia (Sakhalin and Kuril Islands; Figure 4b; Figure 5b).

The selection of relevant environmental predictors taking into consideration important physiological drivers (e.g., light availability for photosynthesis) resulted in sound model predictions (Fragkopoulou et al., 2021; Sequeira et al., 2018) of high accuracy (average performance of AUC > 0.98 and TSS > 0.92). Stacked-SDMs are widely used for estimates of community composition and can be particularly useful in data-poor regions (Cooper & Soberón, 2018; Jayathilake & Costello,

2020). When combined with dispersal constraints, they can reduce overprediction, a common but often neglected SDMs weakness (Mendes et al., 2020), and outperform macroecological models that lack the ability to predict community composition (e.g., Cooper & Soberón, 2018; Mendes et al., 2020). The species richness models tended to overestimate, but only by about one species compared to the global average predicted species richness. This indicates that the potential niche is often realised at scales of 60 km, where community interactions, such as grazing and competition, as well as temporal fluctuations in occurrence, do not affect the regional scale distribution.

The main environmental predictors shaping the present distribution and defining bioclimatic envelopes of kelp and fucoids, inferred from the models, revealed that temperature, light and wave energy are key predictors defining habitat suitability for 420 species, in agreement with expectations from known habitat requirements (Jayathilake & Costello, 2020, 2021; Wernberg et al., 2019; Wilson et al., 2019). Although physiological thresholds differ among species, our results demonstrate that, overall, favourable conditions for subtidal species were primarily shaped by light availability (kelp: > 0.24 E m^{-2} yr^{-1}; fucoid: >1.11E m^{-2} yr^{-1}) and temperature at the seafloor (kelp: 2.8 - 23.7ºC; fucoid: 9.4 - 28.7ºC); while for intertidal fucoids they were shaped by high wave energy (class 5; Fairley et al., 2020), sea surface temperatures (2.5 - 22.8ºC) and salinity (>16.02 PSS). Environmental drivers such as ice cover, contributed less on average to the models, but had high explanatory power on species that reached high latitude (polar and subpolar) distributional ranges (Figure 1; S3) owing to the detrimental effect of ice scouring over intertidal organisms and light attenuation in the subtidal (Assis et al., 2017a; Krause-Jensen et al., 2012). Similarly, salinity had increased explanatory power for species distributed along sharp salinity gradients, such as in the Baltic Sea (Schubert et al., 2011) or in Hudson Bay (Assis et al., 2014), and the Siberian shelf, receiving the discharge of some of the world's largest rivers. These main drivers predicted kelp and

fucoid biomes matching well-described biogeographical limits, such as those in Baja California (Cavanaugh et al., 2019), Morocco (Assis et al., 2014; Lourenço et al., 2016), South Africa (Anderson et al., 2007), Kalbarri Australia (Wernberg et al., 2013) and the extreme cold environments with low-salinity regimes and extensive ice-coverage of the higher latitudes (Jayathilake & Costello, 2020; Kerswell, 2006; Vieira et al., 2021). Although higher resolution is preferred to accurately detect patchy patterns in the distribution of kelp and fucoids, suitable areas for kelp were predicted to cover ~1,71 million km^2, matching the scale of previous studies (1.5 and 2 million km^2; Jayathilake & Costello, 2020, 2021). Fucoids had a larger predicted suitable habitat area than kelps, covering ~2,57 million km^2, a first global estimate for this group.

The inferred regional species richness (poor-spots and rich-spots) and endemicity patterns at global scales can be linked to biogeographic and evolutionary hypotheses for marine forest species (Harrison & Noss, 2017, Kier et al., 2009). Specifically for kelp, the highest regional species richness was found along the California and Alaska coasts, followed by rich-spots in the Okhotsk and Japan-Korea regions, the North Atlantic and the Arctic (Figure 4). Our findings match phylogenetic hypotheses raised by previous studies that suggested that kelp originated in the North-East Pacific (where higher richness was here predicted), later colonized the North-West Pacific and, after recurrent trans-Arctic passages, invaded and colonized the Arctic and North Atlantic Ocean through the opening of the Bering Sea 5.5 Ma ago (Bolton, 2010; Starko et al., 2019). The high richness found in the North East Atlantic (Figure 4a) can be further explained by the larger number of quaternary refugia, allowing long-term persistence of populations, compared to the North-West Atlantic and the Arctic regions where more extensive coastal ice coverage might have affected populations to a higher degree (Assis et al., 2014, 2017a). The general lower species richness (Figure 4a) found in the southern hemisphere is in agreement with evolutionary hypotheses suggesting that

372 southern hemisphere colonizations were rare and in the Laminariales they only occurred for the
373 genera *Ecklonia-Eisenia*, *Lessonia* and *Laminaria* (Table S5; Bolton, 2010), where only the genus
374 *Lessonia* is endemic to the southern hemisphere. Antarctica in particular, is poor in Laminarian
375 kelp species, but rich in endemic species of the genus *Desmarestia*, namely *Desmarestia*
376 *confervoides*; *D. menziesii*; *D. chordalis* (Figure 4b; Table S6; Bringloe et al., 2020), matching the
377 hypothesis of a southern hemisphere origin of this family (Peters et al., 1997). Antarctica thus
378 appears to have been kept mostly isolated, likely due to permanent coastal sea ice cover along most
379 coastlines and seasonal sea ice expansion, in addition to the possible dispersal barrier represented
380 by the Antarctic Circumpolar Current. Regions of kelp endemism, besides *Desmarestia* species in
381 Antarctica, include New Zealand and Southern Ocean islands, and poor-spots of South America
382 (e.g., *Laminaria abyssalis* in Brazil; *Eisenia galapagensis* in the Galapagos Islands) and South Africa
383 (*Ecklonia maxima* and *Laminaria pallida*). The main kelp endemism region for the northern
384 hemisphere is Eastern Russia (*Saccharina gyrata* and *S. cichorioides f. coriacea*; Figure 4b; Table S6).
385
386 The geographical patterns of richness and endemicity of fucoids differed strongly from kelp and
387 matched well the expectation from the evolutionary history of the many species that comprise the
388 order Fucales, with highest regional species richness in South-East Australia, followed by rich-spots
389 in Indonesia and the North-East Atlantic (Figure 5; Table S5). These findings are in agreement with
390 evolutionary hypotheses inferred for the family Sargassaceae, that comprises over 90% of the
391 Fucales species and therefore dominates the patterns of this group (Table 5; Bringloe et al., 2020).
392 The high richness in the tropics and especially in the Indo-Pacific realm (211 species; Table S5)
393 reflects the cosmopolitan distribution of the species-rich genus *Sargassum* (Bringloe et al., 2020;
394 Yip et al., 2020). *Sargassum* was inferred to have evolved and massively radiated in the island-rich
395 central Indo-Pacific region, and only much later diversified into species in other world regions (Yip

et al. 2020), matching our richness patterns. From there, it colonized the Atlantic where species richness is lower (Table S5). The other two fucoid families with several species are the southern hemisphere Seirococcaceae and the anti-tropically distributed Fucaceae. The latter also evolved in Australasia (Cánovas et al., 2011; Serrão et al., 1999), from where they dispersed to the northern Pacific and, when the Bering Sea opened 3-5.5 Ma ago, colonised the Atlantic Ocean where they diversified into multiple lineages (Cánovas et al., 2011; Coyer et al., 2006; Serrão et al., 1999). Thus, the high species richness predicted by our models in the North Atlantic (25 versus 10 Fucaceae species in the North Pacific; Table S5) agrees with hypotheses of higher speciation due to multiple independent crossings of the Bering Strait (Cánovas et al., 2011). Regions of higher fucoid endemicity include both poor-spots such as the Galapagos Islands (e.g., *Sargassum galapagense*, *S. ecuadoreanum*, *S. setifolium*), Antarctica (e.g., *Cystosphaera jacquinotti*), Arabian Peninsula (e.g., *Sargassum dentifolium*, S. *boveanum*, *S. acinaciforme*) and rich-spots such as Baja California (e.g., *Stephanocystis setchellii*, *S. dioica*, *Sargassum johnstonii*, *S. sinicola*), South Africa (e.g., *Bifurcariopsis capensis*, *Brassicophycus brassicaeformis*, *Cystophora fibrosa*), Japan (e.g., *Sargassum yendoi*, *S. ammophilum*, *Coccophora langsdorfii*), South Australia (e.g., *Cystophora xiphocarpa*, *Carpoglossum confluens*) and New Zealand (e.g., *Durvillaea willana*; Figure 5b; Table S7).

The models had generally high performance but still contain inherent limitations such as potential data gaps and uneven sampling effort at global scales. Observed spatial biases are known, for example, for the southern hemisphere, the tropics or Africa (Taheri et al., 2021), stressing the need for additional sampling. Further, missing information on biotic interactions and abiotic characteristics, such as type of substratum, could improve the models and coverage estimates, but no such data are currently available at global scales (Jayathilake & Costello, 2020; Kusumoto et al., 2020). Hence, the current estimate of area is likely an overestimate, as it assumes that all substrata

420 are suitable to support brown macroalgae, although these are largely restricted to rocky shores or
421 hard substrata, such as coral reefs and other biogenic hard structures. Nevertheless, in our approach
422 we used the most accurate and pruned brown macroalgal dataset available and a combination of
423 well-documented methodological approaches to increase model accuracy and provide insights on
424 the potential species richness patterns (Araújo et al., 2019). In particular, integrating dispersal
425 constraints was a key step to reduce overestimations.
426
427 Our results establish novel and valuable baseline information on kelp and fucoid species richness
428 and endemicity estimates. These can be used to inform conservation, management and mitigation
429 strategies. Considering the potential overestimation of predictions of suitable habitats, our
430 endemism estimates are conservative, therefore identifying actual locations of range-restricted
431 species that are of high conservation value. Conservation priority efforts could be directed both at
432 rich-spots, aiming to protect as much biodiversity as possible (Trebilco et al., 2011) and at poor-
433 spots, where habitat availability and ecological services of coastal ecosystems may depend solely on
434 a few species, especially if those contain endemic, range-restricted species (e.g., the Galapagos
435 Islands, Antarctica, South Africa). The estimates here provided could be used as baseline
436 information in habitat restoration planning or in the current efforts to reduce the global mismatch
437 between marine biodiversity and protected areas, in the scope of the Global Biodiversity
438 Framework (Lindegren et al., 2018; Zhao et al., 2020). This is particularly relevant in the context of
439 present and future climate change. Warming trends and extreme climate events have become
440 longer and more frequent (Oliver et al., 2018), impacting marine forests globally and triggering
441 ecosystem tipping points affecting multiple associated species (Arafeh-Dalmau et al., 2020).
442 Characteristic examples of contractions in the distribution of marine forests by hundreds of
443 kilometres within the last one or two decades, causing significant loss of genetic diversity and / or

ecosystem biodiversity, with no signs of recovery, include Southern Australia in 2011 (Wernberg et al., 2013, Coleman & Wernberg, 2017; Gurgel et al., 2020); California in 2014-2016 (Cavanaugh et al., 2019) and northwest Africa / Iberia (Assis et al., 2017c; Lourenço et al. 2016; Nicastro et al. 2013). Building on this framework, future projections anticipate rapid changes in the marine environment and more extreme events (Oliver *et al.*, 2019), that would further impact the distribution of marine forests and threaten some regions of high genetic diversity (Assis et al., 2017a). Therefore, upcoming initiatives should combine our results with future climate projections to flag areas where brown macroalgal forests may be threatened with climate change, contributing to timely consideration of potential conservation and mitigation actions.

Figures

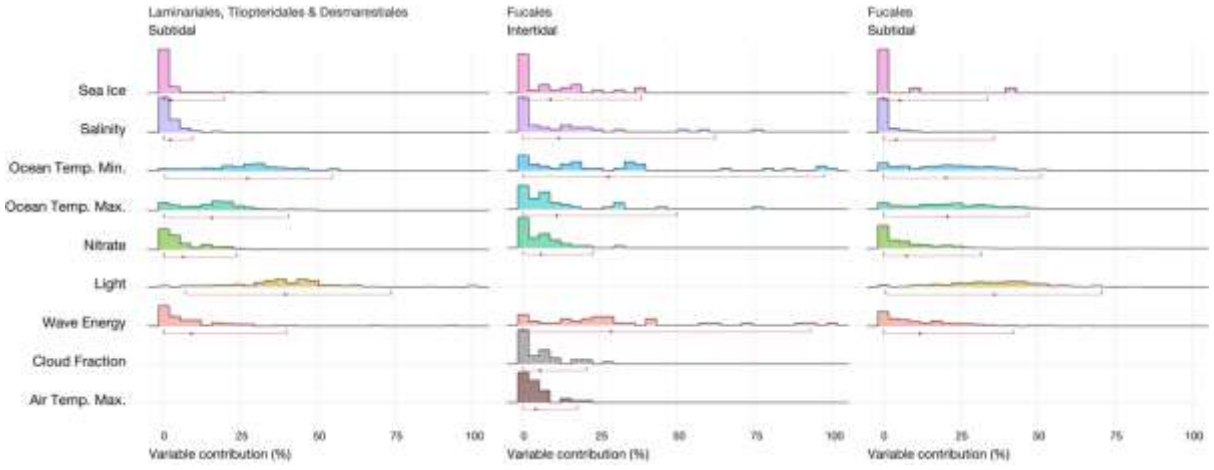

Figure 1. Relative contribution (%) of each environmental predictor to the performance of models for marine forests of (a) kelp, (b) intertidal fucoid and (c) subtidal fucoid. Red lines and red square markers indicate the 95th percentile and the average relative contribution of predictors, respectively.

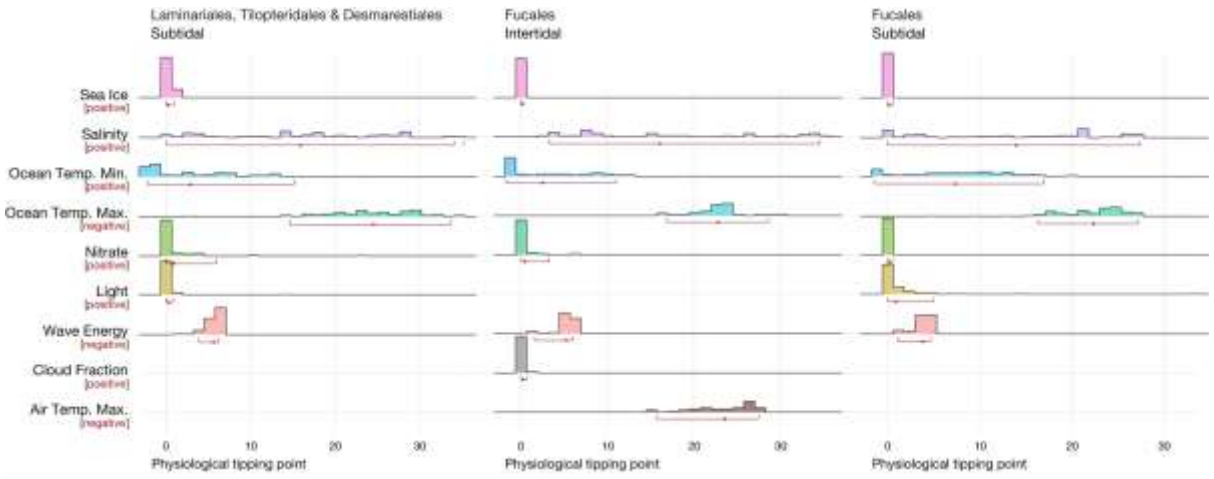

Figure 2. Apparent physiological thresholds inferred from models for marine forests of (a) kelp, (b) intertidal fucoid and (c) subtidal fucoid. Thresholds reflect tolerance limits that can be on the lower (positive) or upper (negative) values of the predictor's gradient. Region defined by red lines and red square marker, indicate the 95th percentile and the average relative contribution of predictors, respectively.

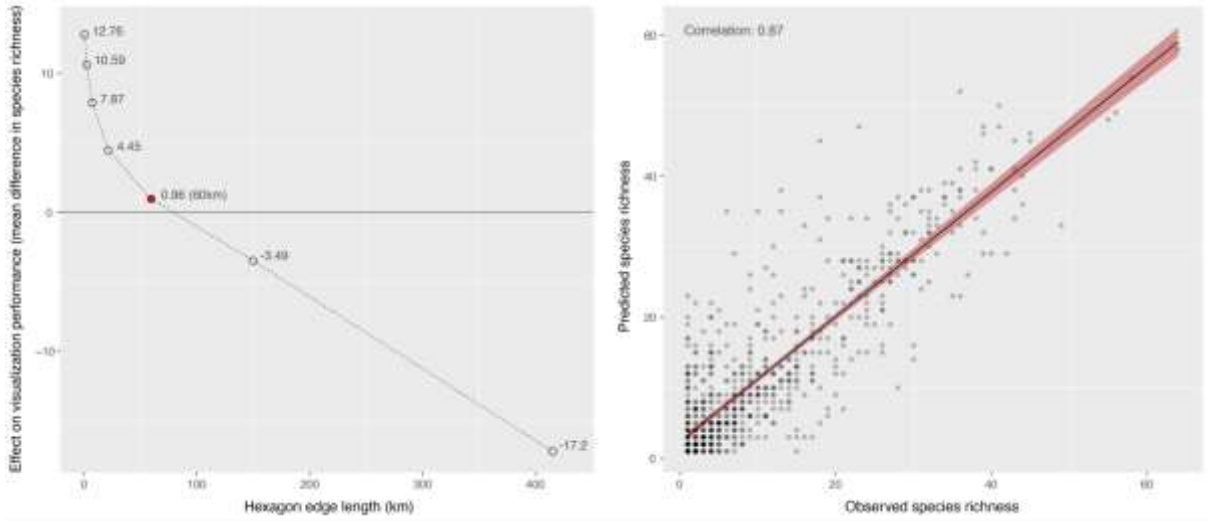

Figure 3. (a) Difference between observed and predicted species richness in relation to the

resolution of hexagon shapes. (b) Correlation between observed and predicted potential species richness at the optimal resolution of hexagon shapes (60 km).

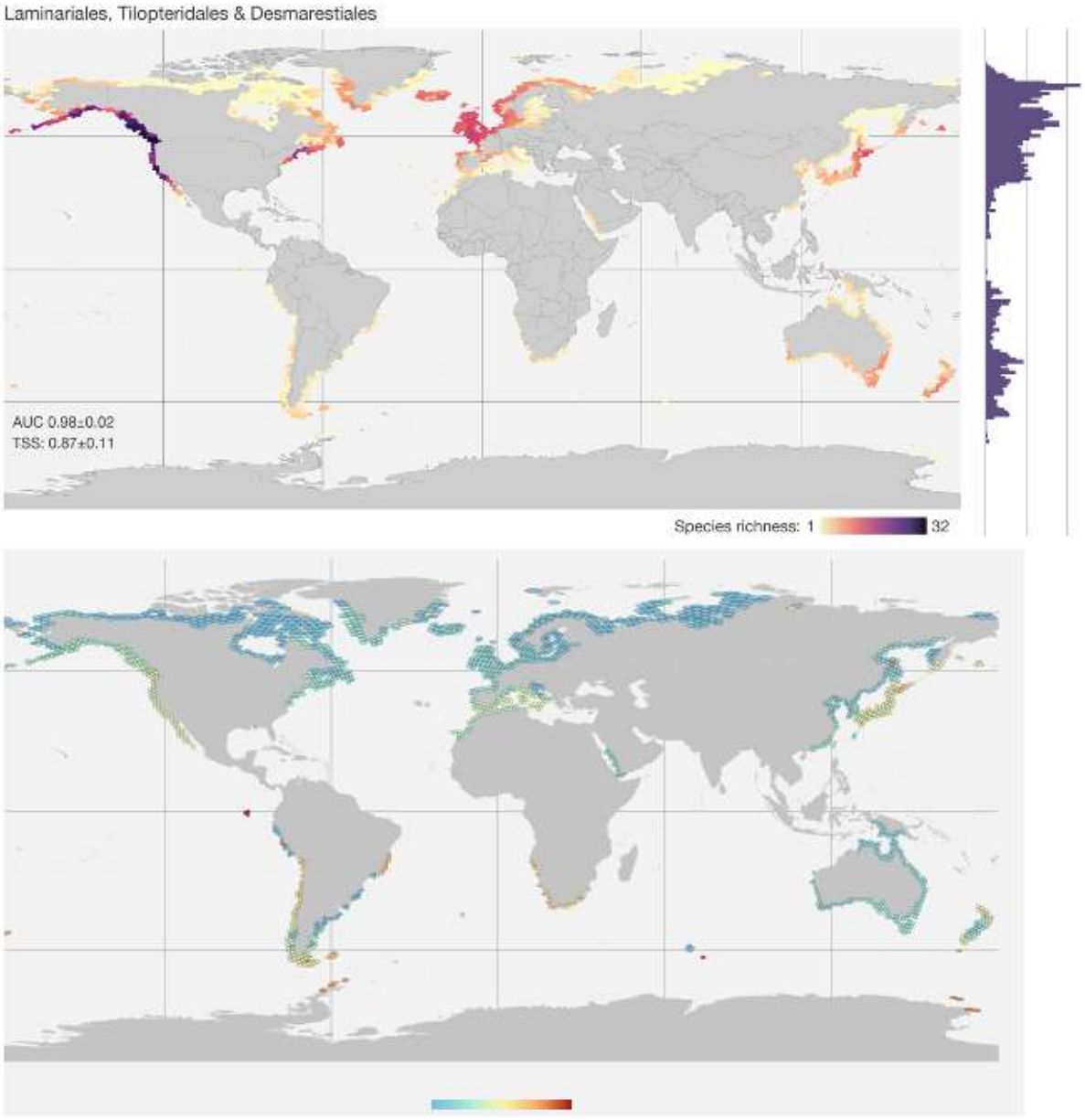

Figure 4. Global estimates of kelp (a) species richness and (b) endemicity for an optimal resolution of the global hexagon grid system (60km). Total suitable habitat area determined with latitudinal bins of 0.5º resolution is presented on the side graphs.

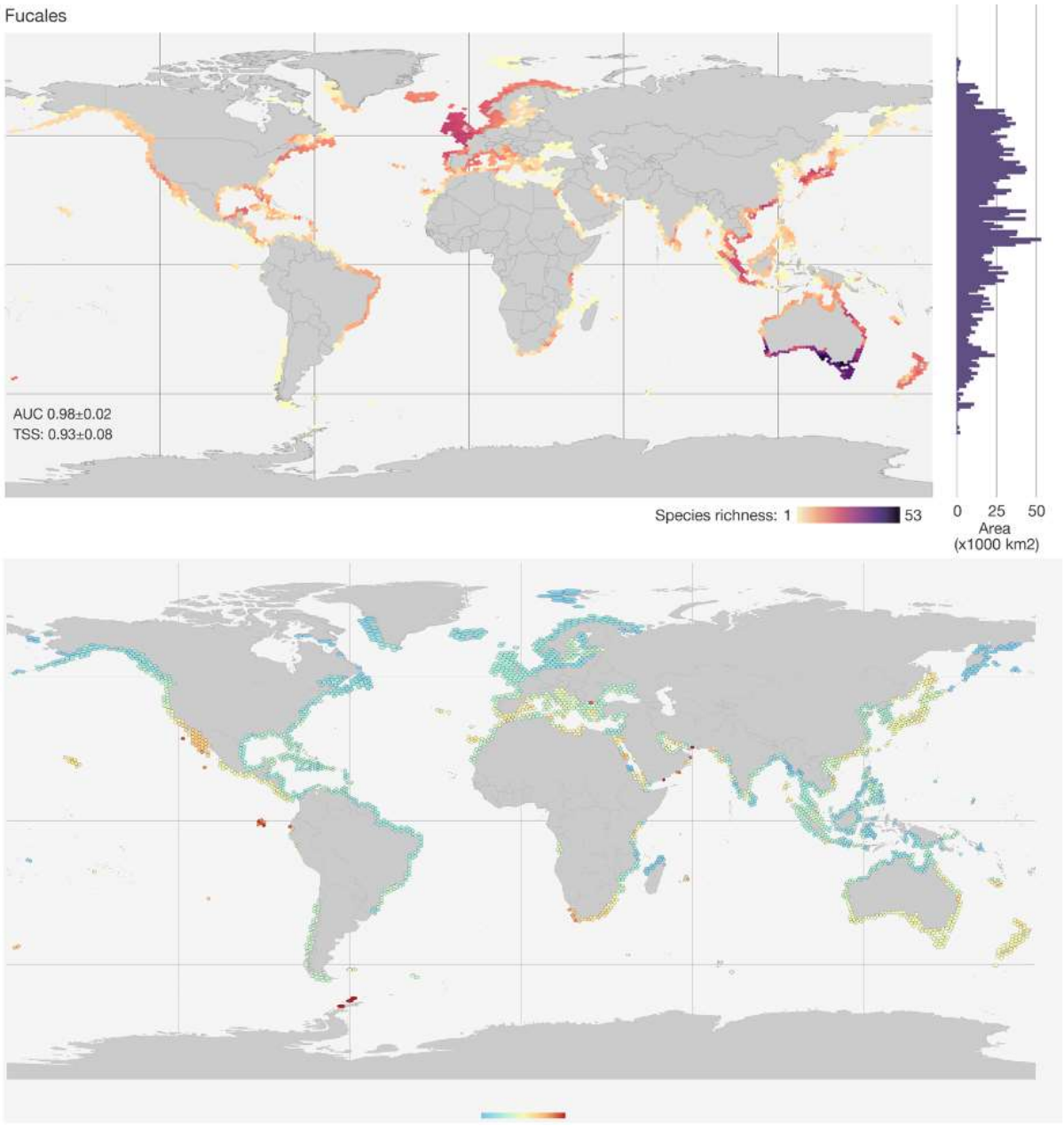

Figure 5. Global estimates of fucoid (a) species richness and (b) endemicity for an optimal resolution of the global hexagon grid system (60km). Total suitable habitat area determined with latitudinal bins of 0.5º resolution is presented on the side graphs.

Supplementary information

S1. List of modelled species and individual number of records.

S2. Predictive performance per modelled species.

S3. Contribution of environmental predictors and apparent physiological thresholds per species.

S4. Collinearity analyses between environmental predictors.

S5. Predicted species richness per family and suitable habitat areas for fucoid and kelp per realm as defined by Spalding et al., (2007).

S6. List of predicted species of kelp per ecoregion as defined by Spalding et al., (2007).

S7. List of predicted species of fucoids per ecoregion as defined by Spalding et al., (2007).

S8. Predictive layers per species and stacked as global estimates of potential species richness (Figshare: https://doi.org/10.6084/m9.figshare.14496018.v1)

Data availability statement

The authors declare that all occurrence and environmental data sources are described in the Material and Methods section. Predictive layers per species and stacked species distribution estimates are available at https://doi.org/10.6084/m9.figshare.14496018.v1. Additional information on models' predictive performance and species richness estimates are provided as supplementary information.

Acknowledgments

This study was supported by the Foundation for Science and Technology (FCT) of Portugal through projects UID/Multi/04326/2020 and PTDC/BIA-CBI/6515/2020. JA was supported by the

transitional norm - DL57/2016/CP1361/CT0035, EF by the fellowship SFRH/BD/144878/2019 and EAS by a Pew Marine Fellowship. DKJ was supported by the Independent Research Fund Denmark (8021-00222 B, "CARMA").

References

Allouche, O., Tsoar, A., & Kadmon, R. (2006). Assessing the accuracy of species distribution models: Prevalence, kappa and the true skill statistic (TSS). *Journal of Applied Ecology*, *43*(6), 1223–1232. https://doi.org/10.1111/j.1365-2664.2006.01214.x

Anderson, R., Rand, A., Rothman, M., Share, A., & Bolton, J. (2007). Mapping and quantifying the South African kelp resource. *African Journal of Marine Science*, *29*(3), 369–378. https://doi.org/10.2989/AJMS.2007.29.3.5.335

Anderson, R. P., Martínez-Meyer, E., Nakamura, M., Araújo, M. B., Peterson, A. T., Soberón, J., & Pearson, R. G. (2011). Ecological Niches and Geographic Distributions. In *Ecological Niches and Geographic Distributions* (Issue December 2016). Princeton University Press. https://doi.org/10.1515/9781400840670

Arafeh-Dalmau, N., Schoeman, D. S., Montaño-Moctezuma, G., Micheli, F., Rogers-Bennett, L., Olguin-Jacobson, C., & Possingham, H. P. (2020). Marine heat waves threaten kelp forests. *Science*, *367*(6478), 635.1-635. https://doi.org/10.1126/science.aba5244

Araújo, M. B., Anderson, R. P., Barbosa, A. M., Beale, C. M., Dormann, C. F., Early, R., Garcia, R. A., Guisan, A., Maiorano, L., Naimi, B., O'Hara, R. B., Zimmermann, N. E., & Rahbek, C. (2019). Standards for distribution models in biodiversity assessments. *Science Advances*, *5*(1), 1–12. https://doi.org/10.1126/sciadv.aat4858

Assis, Jorge, Araújo, M. B., & Serrão, E. A. (2017a). Projected climate changes threaten ancient refugia of kelp forests in the North Atlantic. *Global Change Biology*, *24*(1),

1365–2486. https://doi.org/10.1111/gcb.13818

Assis, J., Berecibar, E., Claro, B., Alberto, F., Reed, D., Raimondi, P., & Serrão, E. A. (2017c). Major shifts at the range edge of marine forests: The combined effects of climate changes and limited dispersal. *Scientific Reports*, *7*(February), 1–10. https://doi.org/10.1038/srep44348

Assis, Jorge, Fragkopoulou, E., Frade, D., Neiva, J., Oliveira, A., Abecasis, D., Faugeron, S., & Serrão, E. A. (2020). A fine-tuned global distribution dataset of marine forests. *Scientific Data*, *7*(1), 119. https://doi.org/10.1038/s41597-020-0459-x

Assis, J., Serrão, E. A., Claro, B., Perrin, C., & Pearson, G. A. (2014). Climate-driven range shifts explain the distribution of extant gene pools and predict future loss of unique lineages in a marine brown alga. *Molecular Ecology*, *23*(11), 2797–2810. https://doi.org/10.1111/mec.12772

Assis, Jorge, Tyberghein, L., Bosch, S., Verbruggen, H., Serrão, E. A., & De Clerck, O. (2017b). Bio-ORACLE v2.0: Extending marine data layers for bioclimatic modelling. *Global Ecology and Biogeography*, *27*(3), 277–284. https://doi.org/10.1111/geb.12693

Ballesteros-Mejia, L., Kitching, I. J., Jetz, W., & Beck, J. (2017). Putting insects on the map: near-global variation in sphingid moth richness along spatial and environmental gradients. *Ecography*, *40*(6), 698–708. https://doi.org/10.1111/ecog.02438

Barbet-Massin, M., Jiguet, F., Albert, C. H., & Thuiller, W. (2012). Selecting pseudo-absences for species distribution models: How, where and how many? *Methods in Ecology and Evolution*, *3*(2), 327–338. https://doi.org/10.1111/j.2041-210X.2011.00172.x

Barve, N., Barve, V., Jimenez-Valverde, A., Lira-Noriega, A., Maher, S.P., Peterson, a. T., Soberon, J., Villalobos, F., Jiménez-Valverde, A., Lira-Noriega, A., Maher, S.P., Peterson, a. T., Soberón, J. & Villalobos, F. (2011) The crucial role of the accessible area

554 in ecological niche modeling and species distribution modeling. *Ecological Modelling*,
555 222(11), 1810–1819. https://doi.org/10.1016/j.ecolmodel.2011.02.011
556 Bolton, J. J. (2010). The biogeography of kelps (Laminariales, Phaeophyceae): a global
557 analysis with new insights from recent advances in molecular phylogenetics. *Helgoland*
558 *Marine Research*, *64*(4), 263–279. https://doi.org/10.1007/s10152-010-0211-6
559 Bondaruk, B., Roberts, S. A., & Robertson, C. (2019). Discrete global grid systems:
560 Operational capability of the current state of the art. *CEUR Workshop Proceedings*,
561 *2323*(6).
562 Bringloe, T. T., Starko, S., Wade, R. M., Vieira, C., Kawai, H., De Clerck, O., Cock, J. M.,
563 Coelho, S. M., Destombe, C., Valero, M., Neiva, J., Pearson, G. A., Faugeron, S., Serrão,
564 E. A., & Verbruggen, H. (2020). Phylogeny and Evolution of the Brown Algae. *Critical*
565 *Reviews in Plant Sciences*, *39*(4), 281–321.
566 https://doi.org/10.1080/07352689.2020.1787679
567 Cánovas, F. G., Mota, C. F., Serrão, E. A., & Pearson, G. A. (2011). Driving south: A multi-
568 gene phylogeny of the brown algal family Fucaceae reveals relationships and recent
569 drivers of a marine radiation. *BMC Evolutionary Biology*, *11*(1).
570 https://doi.org/10.1186/1471-2148-11-371
571 Cavanaugh, K. C., Reed, D. C., Bell, T. W., Castorani, M. C. N., & Beas-Luna, R. (2019).
572 Spatial variability in the resistance and resilience of giant kelp in southern and Baja
573 California to a multiyear heatwave. *Frontiers in Marine Science*, *6*(JUL), 1–14.
574 https://doi.org/10.3389/fmars.2019.00413
575 Chaudhary, C., Saeedi, H., & Costello, M. J. (2016). Bimodality of Latitudinal Gradients in
576 Marine Species Richness. *Trends in Ecology and Evolution*, *31*(9), 670–676.
577 https://doi.org/10.1016/j.tree.2016.06.001

578 Coleman, M. A., & Wernberg, T. (2017). Forgotten underwater forests: The key role of
579 fucoids on Australian temperate reefs. *Ecology and Evolution*, *7*(20), 8406–8418.
580 https://doi.org/10.1002/ece3.3279
581 Cooper, J. C., & Soberón, J. (2018). Creating individual accessible area hypotheses improves
582 stacked species distribution model performance. *Global Ecology and Biogeography*,
583 *27*(1), 156–165. https://doi.org/10.1111/geb.12678
584 Costello, M. J., Tsai, P., Wong, P. S., Cheung, A. K. L., Basher, Z., & Chaudhary, C. (2017).
585 Marine biogeographic realms and species endemicity. *Nature Communications*, *8*(1), 1–
586 9. https://doi.org/10.1038/s41467-017-01121-2
587 Coyer, J. A., Hoarau, G., Oudot-Le Secq, M. P., Stam, W. T., & Olsen, J. L. (2006). A mtDNA-
588 based phylogeny of the brown algal genus Fucus (Heterokontophyta; Phaeophyta).
589 *Molecular Phylogenetics and Evolution*, *39*(1), 209–222.
590 https://doi.org/10.1016/j.ympev.2006.01.019
591 Crisp, M. D., Laffan, S., Linder, H. P., & Monro, A. (2001). Endemism in the Australian
592 flora. *Journal of Biogeography*, 28(2), 183–198. https://doi.org/10.1046/j.1365-
593 2699.2001.00524.x
594 De'ath, G. (2007). Boosted trees for ecological modeling and prediction. *Ecology*, *88*(1), 243–
595 251. https://doi.org/10.1890/0012-9658(2007)88[243:BTFEMA]2.0.CO;2
596 Dormann, C. F., Elith, J., Bacher, S., Buchmann, C., Carl, G., Carré, G., Marquéz, J. R. G.,
597 Gruber, B., Lafourcade, B., Leitão, P. J., Münkemüller, T., Mcclean, C., Osborne, P. E.,
598 Reineking, B., Schröder, B., Skidmore, A. K., Zurell, D., & Lautenbach, S. (2013).
599 Collinearity: A review of methods to deal with it and a simulation study evaluating
600 their performance. *Ecography*, *36*(1), 27–46. https://doi.org/10.1111/j.1600-
601 0587.2012.07348.x

Dormann, C., M. McPherson, J., B. Araújo, M., Bivand, R., Bolliger, J., Carl, G., G. Davies, R., Hirzel, A., Jetz, W., Daniel Kissling, W., Kühn, I., Ohlemüller, R., R. Peres-Neto, P., Reineking, B., Schröder, B., M. Schurr, F., & Wilson, R. (2007). Methods to account for spatial autocorrelation in the analysis of species distributional data: A review. *Ecography*, *30*(5), 609–628. https://doi.org/10.1111/j.2007.0906-7590.05171.x

Elith, Jane, H. Graham, C., P. Anderson, R., Dudík, M., Ferrier, S., Guisan, A., J. Hijmans, R., Huettmann, F., R. Leathwick, J., Lehmann, A., Li, J., G. Lohmann, L., A. Loiselle, B., Manion, G., Moritz, C., Nakamura, M., Nakazawa, Y., McC. M. Overton, J., Townsend Peterson, A., … E. Zimmermann, N. (2006). Novel methods improve prediction of species' distributions from occurrence data. *Ecography*, *29*(2), 129–151.

Elith, Jane, Leathwick, J. R., & Hastie, T. (2008). A working guide to boosted regression trees. In *Journal of Animal Ecology* (Vol. 77, Issue 4, pp. 802–813). https://doi.org/10.1111/j.1365-2656.2008.01390.x

Fairley, I., Lewis, M., Robertson, B., Hemer, M., Masters, I., Horrillo-Caraballo, J., Karunarathna, H., & Reeve, D. E. (2020). A classification system for global wave energy resources based on multivariate clustering. *Applied Energy*, *262*(October 2019), 114515. https://doi.org/10.1016/j.apenergy.2020.114515

Fielding, A. H., & Bell, J. F. (1997). A review of methods for the assessment of prediction errors in conservation presence/absence models. *Environmental Conservation*, *24*(1), 38–49. https://doi.org/10.1017/S0376892997000088

Fragkopoulou, E., Serrão, E. A., Horta, P. A., Koerich, G., & Assis, J. (2021). Bottom Trawling Threatens Future Climate Refugia of Rhodoliths Globally. *Frontiers in Marine Science*, *7*(January), 1–11. https://doi.org/10.3389/fmars.2020.594537

García-Callejas, D., & Araújo, M. B. (2016). of Model and Data Complexity on Predictions

From Species Distributions Models. *Ecological Modelling*, *326*, 4–12. https://doi.org/10.1016/j.ecolmodel.2015.06.002

Guisan, A., & Rahbek, C. (2011). SESAM - a new framework integrating macroecological and species distribution models for predicting spatio-temporal patterns of species assemblages. *Journal of Biogeography*, *38*(8), 1433–1444. https://doi.org/10.1111/j.1365-2699.2011.02550.x

Gurgel, C. F. D., Camacho, O., Minne, A. J. P., Wernberg, T., & Coleman, M. A. (2020). Marine Heatwave Drives Cryptic Loss of Genetic Diversity in Underwater Forests. *Current Biology*, *30*(7), 1199-1206.e2. https://doi.org/10.1016/j.cub.2020.01.051

Harisena, N. V., Groen, T. A., Toxopeus, A. G., & Naimi, B. (2021). When is variable importance estimation in species distribution modelling affected by spatial correlation? *Ecography*, 1–11. https://doi.org/10.1111/ecog.05534

Harrison, S., & Noss, R. (2017). Endemism hotspots are linked to stable climatic refugia. *Annals of Botany*, *119*(2), 207–214. https://doi.org/10.1093/aob/mcw248

Hofner, B., Müller, J., & Hothorn, T. (2011). Monotonicity-constrained species distribution models. *Ecology*, *92*(10), 1895–1901. https://doi.org/10.1890/10-2276.1

Jayathilake, D. R. M., & Costello, M. J. (2020). A modelled global distribution of the kelp biome. *Biological Conservation*, *252*(2020), 108815. https://doi.org/10.1016/j.biocon.2020.108815

Jayathilake, D. R. M., & Costello, M. J. (2021). Version 2 of the world map of laminarian kelp benefits from more Arctic data and makes it the largest marine biome. *Biological Conservation*, *xxx*(April), 109099. https://doi.org/10.1016/j.biocon.2021.109099

Keith, S. A., Kerswell, A. P., & Connolly, S. R. (2014). Global diversity of marine macroalgae: Environmental conditions explain less variation in the tropics. *Global Ecology and*

650 *Biogeography*, *23*(5), 517–529. https://doi.org/10.1111/geb.12132
651 Kerswell, A. P. (2006). Global biodiversity patterns of benthic marine algae. *Ecology*, *87*(10),
652 2479–2488. https://doi.org/10.1890/0012-9658(2006)87[2479:GBPOBM]2.0.CO;2
653 Kier, G., Kreft, H., Tien, M. L., Jetz, W., Ibisch, P. L., Nowicki, C., Mutke, J., & Barthlott, W.
654 (2009). A global assessment of endemism and species richness across island and
655 mainland regions. *Proceedings of the National Academy of Sciences of the United*
656 *States of America*, *106*(23), 9322–9327. https://doi.org/10.1073/pnas.0810306106
657 Krause-Jensen, D., Lavery, P., Serrano, O., Marba, N., Masque, P., & Duarte, C. M. (2018).
658 Sequestration of macroalgal carbon: The elephant in the Blue Carbon room. *Biology*
659 *Letters*, *14*(6). https://doi.org/10.1098/rsbl.2018.0236
660 Krause-Jensen, D., Marbà, N., Olesen, B., Sejr, M. K., Christensen, P. B., Rodrigues, J.,
661 Renaud, P. E., Balsby, T. J. S., & Rysgaard, S. (2012). Seasonal sea ice cover as principal
662 driver of spatial and temporal variation in depth extension and annual production of
663 kelp in Greenland. *Global Change Biology*, *18*(10), 2981–2994.
664 https://doi.org/10.1111/j.1365-2486.2012.02765.x
665 Kusumoto, B., Costello, M. J., Kubota, Y., Shiono, T., Wei, C. L., Yasuhara, M., & Chao, A.
666 (2020). Global distribution of coral diversity: Biodiversity knowledge gradients related
667 to spatial resolution. *Ecological Research*, *35*(2), 315–326. https://doi.org/10.1111/1440-
668 1703.12096
669 Lin, H. Y., Corkrey, R., Kaschner, K., Garilao, C., & Costello, M. J. (2020). Latitudinal
670 diversity gradients for five taxonomic levels of marine fish in depth zones. *Ecological*
671 *Research*, *October*, 1–15. https://doi.org/10.1111/1440-1703.12193
672 Lindegren, M., Holt, B. G., MacKenzie, B. R., & Rahbek, C. (2018). A global mismatch in the
673 protection of multiple marine biodiversity components and ecosystem services.

674 *Scientific Reports*, *8*(1), 1–8. https://doi.org/10.1038/s41598-018-22419-1
675 Lourenço, C. R., Zardi, G. I., McQuaid, C. D., Serrão, E. A., Pearson, G. A., Jacinto, R., &
676 Nicastro, K. R. (2016). Upwelling areas as climate change refugia for the distribution
677 and genetic diversity of a marine macroalga. *Journal of Biogeography*, *43*(8), 1595–
678 1607. https://doi.org/10.1111/jbi.12744
679 Mendes, P., Velazco, S. J. E., de Andrade, A. F. A., & De Marco, P. (2020). Dealing with
680 overprediction in species distribution models: How adding distance constraints can
681 improve model accuracy. *Ecological Modelling*, *431*(August 2019), 109180.
682 https://doi.org/10.1016/j.ecolmodel.2020.109180
683 Nicastro, K. R., Zardi, G. I., Teixeira, S., Neiva, J., Serrão, E. A., & Pearson, G. A. (2013). Shift
684 happens: Trailing edge contraction associated with recent warming trends threatens a
685 distinct genetic lineage in the marine macroalga Fucus vesiculosus. *BMC Biology*, *11,* 6.
686 https://doi.org/10.1186/1741-7007-11-6
687 Oliver, E. C. J., Burrows, M. T., Donat, M. G., Sen Gupta, A., Alexander, L. V., Perkins-
688 Kirkpatrick, S. E., Benthuysen, J. A., Hobday, A. J., Holbrook, N. J., Moore, P. J.,
689 Thomsen, M. S., Wernberg, T., & Smale, D. A. (2019). Projected Marine Heatwaves in
690 the 21st Century and the Potential for Ecological Impact. *Frontiers in Marine Science*,
691 *6*(December), 1–12. https://doi.org/10.3389/fmars.2019.00734
692 Oliver, E. C. J., Donat, M. G., Burrows, M. T., Moore, P. J., Smale, D. A., Alexander, L. V.,
693 Benthuysen, J. A., Feng, M., Sen Gupta, A., Hobday, A. J., Holbrook, N. J., Perkins-
694 Kirkpatrick, S. E., Scannell, H. A., Straub, S. C., & Wernberg, T. (2018). Longer and
695 more frequent marine heatwaves over the past century. *Nature Communications*, *9*(1),
696 1–12. https://doi.org/10.1038/s41467-018-03732-9
697 Pecl, G. T., Araújo, M. B., Bell, J. D., Blanchard, J., Bonebrake, T. C., Chen, I. C., Clark, T. D.,

Colwell, R. K., Danielsen, F., Evengård, B., Falconi, L., Ferrier, S., Frusher, S., Garcia, R. A., Griffis, R. B., Hobday, A. J., Janion-Scheepers, C., Jarzyna, M. A., Jennings, S., … Williams, S. E. (2017). Biodiversity redistribution under climate change: Impacts on ecosystems and human well-being. *Science*, *355*(6332). https://doi.org/10.1126/science.aai9214

Peters, A. F., Oppen, M. J. H., Wiencke, C., Stam, W. T., & Olsen, J. L. (1997). Phylogeny and historical ecology of the desmarestiaceae (phaeophyceae) support a southern hemisphere origin. *Journal of Phycology*, *33*(2), 294–309. https://doi.org/10.1111/j.0022-3646.1997.00294.x

van Proosdij, A. S. J., Sosef, M. S. M., Wieringa, J. J., & Raes, N. (2016). Minimum required number of specimen records to develop accurate species distribution models. *Ecography*, *39*(6), 542–552. https://doi.org/10.1111/ecog.01509

Randin, C. F., Dirnböck, T., Dullinger, S., Zimmermann, N. E., Zappa, M., & Guisan, A. (2006). Are niche-based species distribution models transferable in space? *Journal of Biogeography*, *33*(10), 1689–1703. https://doi.org/10.1111/j.1365-2699.2006.01466.x

Romdal, T. S., Araújo, M. B., & Rahbek, C. (2013). Life on a tropical planet: Niche conservatism and the global diversity gradient. *Global Ecology and Biogeography*, *22*(3), 344–350. https://doi.org/10.1111/j.1466-8238.2012.00786.x

Schmitt, S., Pouteau, R., Justeau, D., de Boissieu, F., & Birnbaum, P. (2017). ssdm: An r package to predict distribution of species richness and composition based on stacked species distribution models. *Methods in Ecology and Evolution*, *8*(12), 1795–1803. https://doi.org/10.1111/2041-210X.12841

Schubert, H., Feuerpfeil, P., Marquardt, R., Telesh, I., & Skarlato, S. (2011). Macroalgal diversity along the Baltic Sea salinity gradient challenges Remane's species-minimum

722 concept. *Marine Pollution Bulletin*, *62*(9), 1948–1956.
723 https://doi.org/10.1016/j.marpolbul.2011.06.033
724 Selig, E. R., Turner, W. R., Troëng, S., Wallace, B. P., Halpern, B. S., Kaschner, K., Lascelles,
725 B. G., Carpenter, K. E., & Mittermeier, R. A. (2014). Global priorities for marine
726 biodiversity conservation. *PLoS ONE*, *9*(1), 1–11.
727 https://doi.org/10.1371/journal.pone.0082898
728 Sequeira, A. M. M., Bouchet, P. J., Yates, K. L., Mengersen, K., & Caley, M. J. (2018).
729 Transferring biodiversity models for conservation: Opportunities and challenges.
730 *Methods in Ecology and Evolution*, *9*(5), 1250–1264. https://doi.org/10.1111/2041-
731 210X.12998
732 Serrão, E. A., Alice, L. A., & Brawley, S. H. (1999). Evolution of the Fucaceae
733 (Phaeophyceae) inferred from nrDNA-ITS. *Journal of Phycology*, *35*(2), 382–394.
734 https://doi.org/10.1046/j.1529-8817.1999.3520382.x
735 Spalding, M. D., Fox, H. E., Allen, G. R., Davidson, N., Ferdaña, Z. A., Finlayson, M., Halpern, B. S.,
736 Jorge, M. A., Lombana, A., Lourie, S. A., Martin, K. D., Mcmanus, E., Molnar, J., Recchia, C. A.,
737 & Robertson, J. (2007). Marine Ecoregions of the World: A Bioregionalization of coastal and
738 shelf areas. *Bioscience*, *57*(7), 573. Https://Doi.Org/10.1641/B570707
739 Starko, S., Soto Gomez, M., Darby, H., Demes, K. W., Kawai, H., Yotsukura, N., Lindstrom, S. C.,
740 Keeling, P. J., Graham, S. W., & Martone, P. T. (2019). A comprehensive kelp phylogeny sheds
741 light on the evolution of an ecosystem. *Molecular Phylogenetics and Evolution*, *136*(April),
742 138–150. https://doi.org/10.1016/j.ympev.2019.04.012
743 Taheri, S., Naimi, B., Rahbek, C., & Araújo, M. B. (2021). Improvements in reports of species
744 redistribution under climate change are required. *Science Advances*, *7*(15), eabe1110.
745 https://doi.org/10.1126/sciadv.abe1110

Thuiller, W., Brotons, L., Araújo, M. B., & Lavorel, S. (2004). Effects of restricting environmental range of data to project current and future species distributions. *Ecography*, *27*(2), 165–172. https://doi.org/10.1111/j.0906-7590.2004.03673.x

Tittensor, D. P., Mora, C., Jetz, W., Lotze, H. K., Ricard, D., Berghe, E. Vanden, & Worm, B. (2010). Global patterns and predictors of marine biodiversity across taxa. *Nature*, *466*(7310), 1098–1101. https://doi.org/10.1038/nature09329

Trebilco, R., Halpern, B. S., Mills, J., Field, C., Blanchard, W., & Worm, B. (2011). Mapping species richness and human impact drivers to inform global pelagic conservation prioritisation. *Biological Conservation*, *144*(5), 1758–1766. https://doi.org/10.1016/j.biocon.2011.02.024

Tyberghein, L., Verbruggen, H., Pauly, K., Troupin, C., Mineur, F., & De Clerck, O. (2012). Bio-ORACLE: A global environmental dataset for marine species distribution modelling. *Global Ecology and Biogeography*, *21*(2), 272–281. https://doi.org/10.1111/j.1466-8238.2011.00656.x

Verbruggen, H., Tyberghein, L., Pauly, K., Vlaeminck, C., Nieuwenhuyze, K. Van, Kooistra, W. H. C. F., Leliaert, F., & de Clerck, O. (2009). Macroecology meets macroevolution: Evolutionary niche dynamics in the seaweed Halimeda. *Global Ecology and Biogeography*, *18*(4), 393–405. https://doi.org/10.1111/j.1466-8238.2009.00463.x

Vieira, C., Steen, F., D'hondt, S., Bafort, Q., Tyberghein, L., Fernandez-García, C., Wysor, B., Tronholm, A., Mattio, L., Payri, C., Kawai, H., Saunders, G., Leliaert, F., Verbruggen, H., & De Clerck, O. (2021). Global biogeography and diversification of a group of brown seaweeds (Phaeophyceae) driven by clade-specific evolutionary processes. *Journal of Biogeography*. https://doi.org/10.1111/jbi.14047

Vignali, S., Barras, A. G., Arlettaz, R., & Braunisch, V. (2020). SDMtune: An R package to

770 tune and evaluate species distribution models. *Ecology and Evolution*, *10*(20), 11488–
771 11506. https://doi.org/10.1002/ece3.6786
772 Wernberg, T., Krumhansl, K., Filbee-Dexter, K., & Pedersen, M. F. (2019). Status and Trends
773 for the World's Kelp Forests. In *World Seas: an Environmental Evaluation* (Second Edi,
774 pp. 57–78). Elsevier Ltd. https://doi.org/10.1016/B978-0-12-805052-1.00003-6
775 Wernberg, T., Smale, D. A., Tuya, F., Thomsen, M. S., Langlois, T. J., De Bettignies, T.,
776 Bennett, S., & Rousseaux, C. S. (2013). An extreme climatic event alters marine
777 ecosystem structure in a global biodiversity hotspot. *Nature Climate Change*, *3*(1), 78–
778 82. https://doi.org/10.1038/nclimate1627
779 Wiens, J. J., & Donoghue, M. J. (2004). Historical biogeography, ecology and species
780 richness. *Trends in Ecology and Evolution*, *19*(12), 639–644.
781 https://doi.org/10.1016/j.tree.2004.09.011
782 Wilson, K. L., Skinner, M. A., & Lotze, H. K. (2019). Projected 21st-century distribution of
783 canopy-forming seaweeds in the Northwest Atlantic with climate change. *Diversity*
784 *and Distributions*, *25*(4), 582–602. https://doi.org/10.1111/ddi.12897
785 Yip, Z. T., Quek, R. Z. B., & Huang, D. (2020). Historical biogeography of the widespread
786 macroalga Sargassum (Fucales, Phaeophyceae). *Journal of Phycology*, *56*(2), 300–309.
787 https://doi.org/10.1111/jpy.12945
788 Zhao, Q., Stephenson, F., Lundquist, C., Kaschner, K., Jayathilake, D., & Costello, M. J.
789 (2020). Where Marine Protected Areas would best represent 30% of ocean biodiversity.
790 *Biological Conservation*, *244*(July 2019), 108536.
791 https://doi.org/10.1016/j.biocon.2020.108536
792
793